PROCEEDINGS OF SCIENCE

The ATLAS silicon strip detector running experience

Manuel Kayl*, **on behalf of the ATLAS SCT collaboration**
Nikhef, NL
E-mail: mkayl@nikhef.nl

The silicon strip detector (SemiConductor Tracker, SCT) is one of the three sub-detectors of the ATLAS inner tracking system. It was fully installed in the ATLAS cavern and has been commissioned under realistic operation conditions. A large set of cosmic ray data was taken in 2008 with different magnetic field conditions. Besides gaining experience on operating the detector, key detector properties like the noise occupancy and the hit efficiencies as well as the Lorentz angle were studied. Early alignment results and the tracking performance are also discussed in this report.

ATL-INDET-PROC-2009-023
01 December 2009

VERTEX 2009 (18th workshop) - VERTEX 2009
September 13 - 18 2009
Veluwe, the Netherlands

*Speaker.

1. Introduction

ATLAS [1] is a general purpose detector at the Large Hadron Collider (LHC) at CERN, Geneva. The LHC is designed to collide protons at a centre of mass energy of $\sqrt{s} = 14$ TeV and a luminosity of 10^{34} cm^{-2} s^{-1}. The total cross section at the LHC is expected to be roughly 100 mb [2]. The unprecedented energy and luminosity of the LHC imposes tight constraints and requirements on the layout of the detectors: high granularity, fast readout and a high radiation hardness are needed. The Inner Detector (ID) is the innermost tracking device of ATLAS located in a 2 T solenoid magnet. The ID consists of a silicon pixel detector, a silicon strip detector and a straw tube transition radiation tracker (TRT). Its main design goals are the primary and secondary vertex identification as well as a precise momentum measurement of high energy particles in the region $|\eta| < 2.5$.

2. The SemiConductor Tracker (SCT)

The silicon strip detector is called SemiConductor Tracker (SCT) and is located between the Pixel and TRT detectors. It consists of a barrel and two end-cap detectors as can be seen in Figure 1. The barrel is made of four cylindrical layers containing 2112 modules, each endcap is made of nine radial disks containing 988 modules each. Depending on the particular layer the barrel covers $|\eta| < 1.1$ to 1.4 and the end-caps cover the region up to $|\eta| < 2.5$.

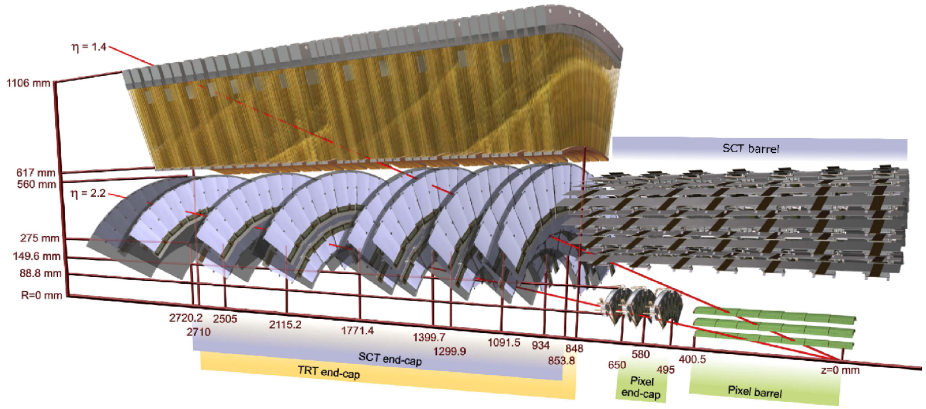

Figure 1: Drawing of the ATLAS Inner Detector traversed by two 10 GeV tracks with $\eta = 1.4$ and 2.2. The TRT barrel detector is not shown.

The SCT modules [3, 4] consist of two sensors glued back-to-back which are rotated by a stereo angle of 40 mrad with respect to each other. The sensors are constructed using p-type readout strips on n-type bulk silicon. The strip pitch is 80 μm in the barrel and varies in the end-caps between 57 μm and 94 μm due to a fan geometry. There are 768 active readout channels per module side. A binary readout with a default threshhold of 1fC is provided by six radiation hard ABCD [5] chips for one module side. For the module communication with the off-detector electronics optical links [6] are used. The conversion of the electronic to optical signal is done via laser diodes (VCSELs).

The modules are operated at reverse bias with an initial voltage of 150 V. To keep the effect of radiation damage within limits the silicon is operated at a temperature of -7 °C. This is realised by means of an evaporative cooling system using C_3F_8 operating at $-25°C$.

Tight requirements are imposed on the performance of the modules. The single hit resolution is required to be 17 μm $\times$ 580 μm in the R-ϕ and z direction while the maximum module-to-module alignment tolerances are 12 μm $\times$ 50 μm. The noise occupancy is required to be smaller than 5×10^{-4} whereas the detector should work with an efficiency of at least 99%. Considering a 10 year operation time the detector is required to withstand a particle fluence of 2×10^{14} Neq cm^{-2}.

3. Commissioning of the SCT with cosmic ray data

The installation of the SCT was completed with the sign-off in early 2008. Subsequently, the commissioning of the SCT began with the participation in several standalone and combined data taking periods. In particular between October and December 2008 a large sample of cosmic ray data was recorded with the whole ATLAS detector. During this period approximately 2 million tracks traversing the SCT were collected with and without magnetic field. However, since cosmic muons in general do not traverse the nominal interaction region of the detector, several discrepancies with respect to collision data taking have to be considered. The track parameter distributions such as the momentum spectrum or the angular distributions differ significantly. A single cosmic muon traverses the upper and lower half of the detector, see Figure 2. Moreover, the end-caps are poorly illuminated and cannot be commissioned to the same level as the barrel.

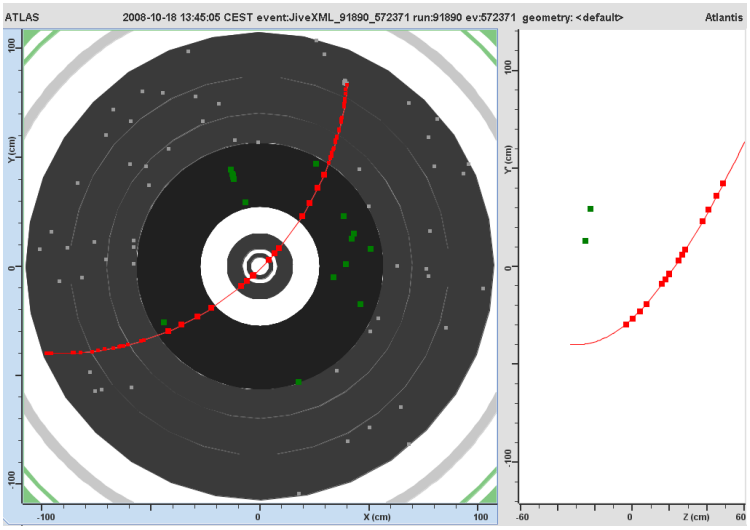

Figure 2: An event display (right) of a reconstructed track from a cosmic muon producing hits in the ID.

3.1 Noise occupancy

The noise occupancy is a crucial property of tracking detectors since hits caused by noise will be included in the pattern recognition and may eventually lead to inefficient tracking algorithms.

The noise occupancy N_{strip} per readout strip during physics data taking is given as

$$N_{strip} = \frac{N_{hits} - N_{SpacePointHits}}{N_{events} - N_{SpacePointHits}}, \tag{3.1}$$

where N_{events} is the number of analysed events, N_{hits} is the number of events with a hit recorded on the strip and $N_{SpacePointHits}$ is the number of recorded hits that were used to produce a track. Figure 3 (left) shows the noise occupancy averaged over a readout chip (128 channels) of the barrel and end-caps for different module types. Modules where the noise occupancy test failed are excluded from the analysis. The noise occupancy depends on the operation temperature and the length of the strips. The readout chips shown meet the specification of a noise occupancy smaller than 5×10^{-4}.

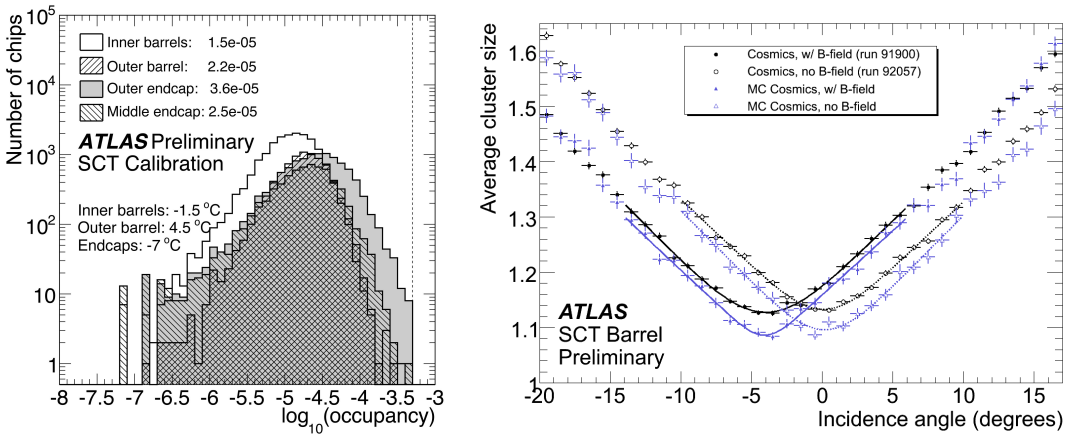

Figure 3: Left plot: noise occupancy in barrel and end-cap detectors. The dashed line represents the specification limit. Right plot: the Lorentz angle measurement with and without magnetic field obtained from data and simulation.

3.2 Measurement of the Lorentz angle

In the presence of a magnetic field the drift path of the charge carriers inside a silicon detector is deflected due to the Lorentz force. The resulting Lorentz angle is an important quantity the track finding algorithms have to take into account. The average cluster size as a function of incidence angle is shown in Figure 3 (right) for data and simulation events with and without magnetic field. The Lorentz angle is roughly determined as the incidence angle at the minimal average cluster size. As expected, the minimum is at 0 in the case without magnetic field and shifted for events recorded with magnetic field. The Lorentz angle is measured on data to be $\Theta_L = 3.93 \pm 0.03\ (stat.) \pm 0.10\ (syst.)$ degrees, which is in good agreement with simulation ($\Theta_L = 3.69 \pm 0.26\ (syst.)$ degrees). However, the actual cluster size at its minimum is slightly larger in data. The biggest uncertainties of the simulation are the hole drift velocity and the non-uniformity of the electric field in the readout sensors.

3.3 Hit efficiency

The intrinsic hit efficiency is a benchmark number for every tracking detector and does not only reflect the quality of the construction but also the understanding of the detector. Dead chan-

nels, detector calibration, alignment and the track finding procedure will affect the efficiency. Figure 4 shows the efficiencies measured in the barrel and in the end-cap detectors. They are computed as the ratio of the number of hits that are expected by the track finding algorithm and the number of hits actually present. The tracks were required to have at least 10 SCT and 40 TRT hits. Non-operational modules (approximately 1%) are disregarded. Most of barrel layers and end-cap disks reach a level of at least 99% efficiency.

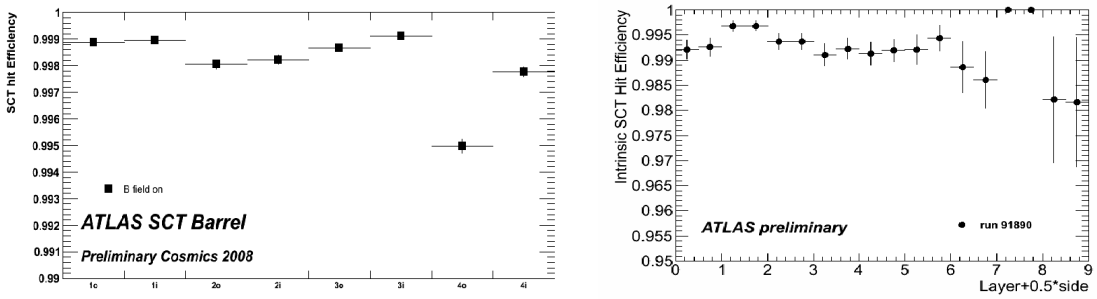

Figure 4: Intrinsic hit efficiencies of the SCT barrel (left) and end-cap (right) as a function of barrel layer or end-caps disk.

3.4 Room for improvements

Although the commissioning is progressing well for the SCT, some problems were encountered. The installation and the operation of the evaporative cooling system were slowed down due to problems with the heater components and the cooling plant. In May 2008 a simultaneous failure of three out of six compressors of the cooling plant occurred. Subsequently the whole cooling plant was replaced and became operational again in August 2008. Two cooling loops of one end-cap were not working, one due to a leak affecting 13 modules in the outermost disk and one due to a damaged cable, which was repaired in early 2009. During operation of the cooling system it was realised that the original design temperature of the modules of -7 °C will not be reached. The modules will be operated at an average temperature of 0 - 5 °C instead.

As mentioned before, VCSELs are used for the generation of optical signals to and from the detector. VCSELs are located near the modules and off-detector in the data acquisition racks on data transmitter boards (TX plug-ins). Problems within the optical transmission system were observed with the TX plug-ins. Electro-Static-Discharges (ESD) during the production seem to be the reason for the high failure rate. No problems were observed with the on-detector devices. A new production of TX plug-ins was launched and all VCSELs were replaced in summer 2009. Furthermore, some modules were affected by HV trips during data taking and needed a reset. An overview of the non-operational readout channels at the end of 2008 together with the number of non-repairable channels is given in Table 1.

4. SCT readiness for collisions

4.1 Alignment

During the early data taking period the alignment will be one the most important and chal-

Detector	Dead at the end of 2008	Not expected to be recovered
Barrel	1.15%	0.19%
End-caps	3.12%	0.93%
Entire SCT	2.10%	0.55%

Table 1: Overview of the dead channels at the end of 2008 and the number of channels that are expected to be non-repairable.

lenging tasks. Substantial information on the alignment of the modules can already be extracted from cosmic ray events. A comparison of the hit residuals obtained before and after the alignment procedure together with the expectation from simulation is shown in Figure 5 for the barrel and end-cap detectors. The distributions were produced from a sample containing data with and without magnetic field. Taking the quadratic difference, the widths of the barrel residual distributions are consistent with a random misalignment of roughly 20 μm. Although the alignment is not yet performed on module but only on disk level, substantial improvement is also achieved in the end-caps.

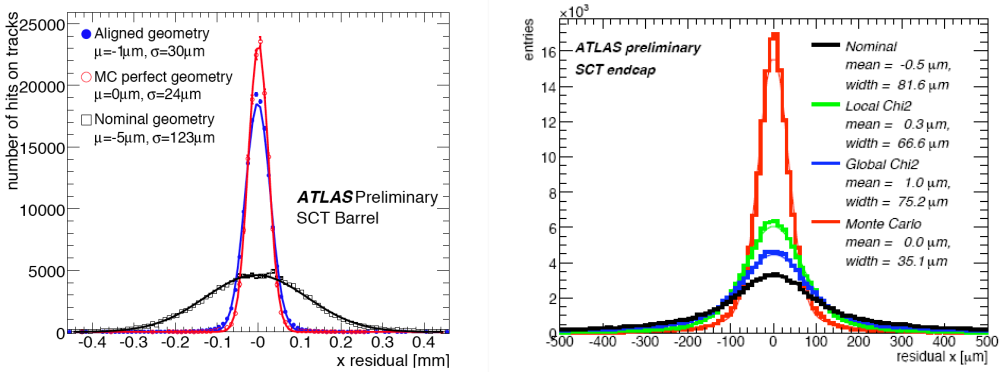

Figure 5: Hit residual distributions before and after the alignment procedure compared to simulation for the barrel (left) and end-cap (right) detectors.

4.2 Tracking performance

Determining the track parameter resolutions is of key importance for all physics analyses. The SCT as the main tracking device plays a major role in these studies. The helical track parameter model [7] consists of five track parameters $\Lambda^T = (d_0, z_0, \phi_0, \theta, q/p)$: the transverse and longitudinal impact parameters, the azimuthal and polar angles as well as the charge-signed inverse momentum.

A fully data-driven method was used to compute the resolutions from cosmic data. Since a cosmic muon traverses the whole detector, the produced hits can be divided in hit collections only containing hits in the upper or lower hemisphere of the detector. These hit collections are refitted separately producing two tracks that resemble tracks from collision events. The difference of their track parameters $\Delta\lambda = \lambda_{up} - \lambda_{low}$ has an expectation value of 0 and a width of $\sigma(\lambda) \times \sqrt{2}$, where $\sigma(\lambda)$ is the resolution of a track parameter.

Figure 6 shows the transverse and longitudinal impact parameter resolutions as a function of transverse momentum. Tracks being reconstructed using all three sub-detectors (full ID) and

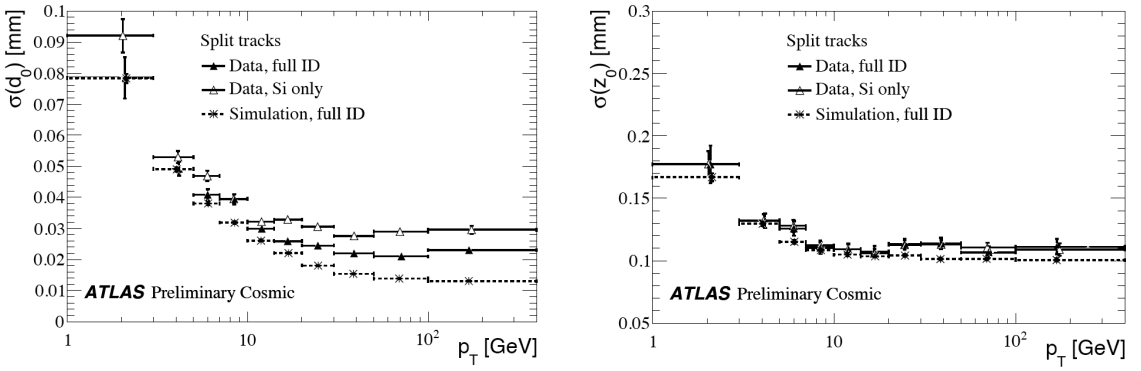

Figure 6: Impact parameter resolutions determined from data and simulation as function of transverse momentum.

only the silicon detectors (Si only) are compared with full ID tracks from simulation. At low momenta the resolution is governed by multiple scattering in the beam pipe, the first pixel layers and infrastructure services of the pixels. For higher momenta, above 10 GeV, the impact parameter resolutions approach the intrinsic detector resolution. The small differences between the data and simulation measurements indicate remaining misalignments in the detector.

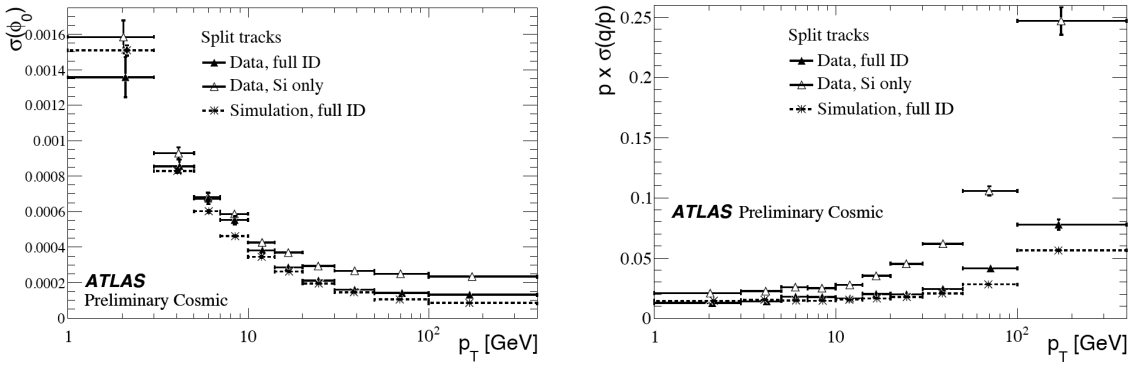

Figure 7: Azimuthal angle and relative momentum resolution determined from data and simulation as function of transverse momentum.

In Figure 7 the azimuthal angle resolution and the relative momentum resolution are displayed as a function of transverse momentum. Similar to the impact parameter resolutions the angular resolution is dominated by multiple scattering in the low p_T region and by the intrinsic detector resolution at higher values of p_T. The relative momentum resolution is better at lower p_T since low energetic particles curve more in the magnetic field which leads to a more precise determination of the curvature and hence the momentum. At high p_T, the contribution of the TRT to the momentum measurement becomes significant. Due to an enlarged lever arm the curvature can be determined more accurately when including the TRT. The remaining differences to the simulation are small and demonstrate the excellent understanding of the detector.

5. Conclusions

The ATLAS SCT detector was commissioned with cosmic ray data taken in autumn 2008. A lot of progress has been made with the calibration of the detector. The measured noise levels and intrinsic hit efficiencies meet the specifications imposed by the challenging operation conditions once the LHC is turned on. A precise determination of the Lorentz angle was carried out and agrees with the expected value from simulation. The remaining uncertainties on the position of the SCT modules are consistent with random module misalignments of roughly 20 μm. The profound understanding of the detector is reflected by the measurement of the track parameter resolutions that show good agreement with the predicted values from simulation. Problems, which were encountered with the evaporative cooling system and the optical transmission systems of the modules, were vastly solved. The results from cosmic ray data taking demonstrate the readiness of the SCT for data taking with collision events.

References

[1] The ATLAS Collaboration, *The ATLAS experiment at the CERN Large Hadron Collider*, JINST 3 (2008) S08003

[2] A. Moraes, C. Buttar and I. Dawson, *Prediction for minimum bias and underlying event at LHC energies*, Eur. Phys. J., C 50:435-466, 2007

[3] A. Abdesselam et al., *The barrel modules of the ATLAS semiconductor tracker*, Nucl. Instrum. Meth. A 568 (2006) 642

[4] A. Abdesselam et al., *The ATLAS semiconductor tracker end-cap module*, Nucl. Instrum. Meth. A 575 (2007) 352

[5] F. Campabadal et al., *Design and performance of the ABCD3TA ASIC for readout silicon strip in the ATLAS semiconductor tracker*, Nucl. Instrum. Meth. A 552 (2005) 561

[6] A. Abdesselam et al., *The optical links of the ATLAS Semi Conductor Tracker*, JINST 2 (2007) P09003

[7] T.G. Cornelissen et al., *Concepts, design and implementation of the ATLAS NewTracking*, ATLAS Note ATL-SOFT-PUB-2007-007